J Mater Sci: Mater Med (2010) 21:2723–2731
DOI 10.1007/s10856-010-4116-3

Study of Pd–Ag dental alloys: examination of effect of casting porosity on fatigue behavior and microstructural analysis

D. Li · N. Baba · W. A. Brantley · S. B. Alapati · R. H. Heshmati · G. S. Daehn

Received: 23 August 2007 / Accepted: 11 June 2010 / Published online: 10 July 2010

Abstract The goals of this study were to investigate the fatigue limits of two Pd–Ag alloys (Ivoclar Vivadent) with differing mechanical properties and varying proportions of secondary alloying elements, examine the effect of casting porosity on fatigue behavior, and determine the effect of casting size on microstructures and Vickers hardness. The alloys selected were: IPS d.SIGN 59 (59.2Pd–27.9Ag–8.2Sn–2.7In–1.3Zn); and IS 64 (59.9Pd–26.0Ag–7.0Sn–2.8Au–1.8 Ga–1.5In–1.0Pt). Tension test bars, heat-treated to simulate dental porcelain application, were subjected to cyclic loading at 10 Hz, with R-ratio of −1 for amplitudes of compressive and tensile stress. Two replicate specimens were tested at each stress amplitude. Fracture surfaces were examined with a scanning electron microscope (SEM). Sectioned fatigue specimens and additional cast specimens simulating copings for a maxillary central incisor restoration were also examined with the SEM, and Vickers hardness was measured using 1 kg load. Casting porosity was evaluated in sectioned fatigue fracture specimens, using an image analysis program. The fatigue limit (2×10^6 loading cycles) of IS 64 was approximately 0.20 of its 0.2% yield strength, while the fatigue limit of d.SIGN 59 was approximately 0.25 of its 0.2% yield strength. These relatively low ratios of fatigue limit to 0.2% yield strength are similar to those found previously for high-palladium dental alloys, and are attributed to their complex microstructures and casting porosity. Complex fatigue fracture surfaces with striations were observed for both alloys. Substantial further decrease in the number of cycles for fatigue failure only occurred when the pore size and volume percentage became excessive. While the heat-treated alloys had equiaxed grains with precipitates, the microstructural homogenization resulting from simulated porcelain firing differed considerably for the coping and fatigue test specimens; the latter specimens had significantly higher values of Vickers hardness.

D. Li · S. B. Alapati
Section of Oral Biology, The Ohio State University, Columbus, OH, USA

N. Baba · W. A. Brantley (✉)
Division of Restorative and Prosthetic Dentistry, College of Dentistry, The Ohio State University, PO Box 182357, Columbus, OH 43218-2357, USA
e-mail: brantley.1@osu.edu; wbrantle@columbus.rr.com

R. H. Heshmati
Division of Primary Care, College of Dentistry, The Ohio State University, Columbus, OH, USA

G. S. Daehn
Department of Materials Science and Engineering, The Ohio State University, Columbus, OH, USA

Present Address:
D. Li
Greatbatch, Inc, Clarence, NY, USA

Present Address:
S. B. Alapati
Department of Endodontics, College of Dentistry, University of Illinois at Chicago, Chicago, IL, USA

1 Introduction

Since their introduction in the early 1970s, Pd–Ag dental casting alloys have been widely used for metal-ceramic restorations and superstructures for implants [1–3]. The properties of Pd–Ag alloys are comparable or superior to gold-based and high-Pd ceramic alloys, and these alloys are economically attractive alternatives for clinical selection. They have acceptable yield strength, excellent ductility, high elastic modulus, high distortion resistance during

porcelain firing, excellent porcelain-metal bond strength, favorable handling properties and solderability, and satisfactory tarnish and corrosion resistance [4–14]. The clinical selection of Pd–Ag alloys has increased because of the alleviation or elimination of former porcelain discoloration concerns by proper melting and casting techniques, selection of particular brands of porcelain, and the incorporation of certain elements in the alloy compositions [1, 3, 15–20].

As almost all restorations are subjected to cyclic forces from mastication, it is necessary to understand the fatigue performance of dental casting alloys. At present, there is no standard for fatigue testing of dental alloys. Using tensile test specimens following ADA Specifications No. 5 [21] and No. 38 [22], which were subjected to clinically relevant heat treatment simulating the process for bonding porcelain, the fatigue limits and fracture characteristics of representative high-Pd [23] and Pd–Ag [24] dental casting alloys were previously determined. The fatigue limits for both types of palladium-based alloys were relatively low, approximately 0.15–0.20 of the 0.2% yield strength in tension. However, these fatigue test specimens were much larger than clinical cast restorations, and it has been found that the microstructures of these specimens may differ from much smaller specimens having the dimensions of clinical restorations [25, 26].

The question arises as to whether fatigue properties for these larger fatigue test specimens are appropriate for clinical restorations. Two purposes of this study were to (a) compare the microstructures and Vickers hardness values of fatigue test specimens and specimens simulating copings for maxillary incisor restorations prepared from two Pd–Ag alloys that had not previously been investigated and (b) study the fatigue limits and fracture characteristics of these alloys. An additional objective of this study was to (c) investigate whether casting porosity in the Pd–Ag alloys had a noteworthy effect on the fatigue limit. In the molten state, Pd–Ag alloys readily absorb atmospheric gases, which can result in substantial porosity in the dental castings since the solubility of these gases is much lower in the solidified alloy [2].

2 Materials and methods

Two Pd–Ag alloys, IS 64 and IPS d.SIGN 59 (Ivoclar Vivadent, Amherst, NY, USA), were selected. Nominal compositions and mechanical properties (after simulated heat treatment for porcelain application) of the alloys are listed in Tables 1 and 2, respectively. The IS 64 alloy has physical properties intended to match those for dental implant superstructures. The IPS d.SIGN 59 alloy (hereafter d.SIGN 59) has mechanical and physical properties that are coordinated with the IPS d.SIGN fluorapatite-leucite glass-ceramic material (Ivoclar Vivadent).

A fine-grained, carbon-free, phosphate-bonded investment (Cera-Fina, Whip-Mix, Louisville, KY, USA) was used to prepare two types of cast specimens. The first type simulated a coping for a maxillary central incisor restoration [26], and wax patterns were used. The second type met the dimensional requirements of ADA Specification Nos. 5 [21] and 38 [22] for tensile test bars, with gauge diameter of 3 mm and gauge length of 15 mm, and polystyrene plastic patterns (Salco, Romeoville, IL, USA) were used. The alloys were melted with a multi-orifice gas-oxygen torch, centrifugally cast using a broken-arm casting machine, and bench-cooled. After divesting, the sprues were cut from the specimens using a carborundum disk, and any visible nodules were removed. The specimens for fatigue testing otherwise had the as-cast surface condition, and were not subsequently air-abraded or polished.

Cast specimens that simulated copings were cross-sectioned into halves, using a slow-speed water-cooled diamond saw (Leco, St. Joseph, MI, USA). One half was used to investigate the as-cast microstructure, and the other half was subjected to the entire heating regimen for application of dental porcelain (Ultra-Mat CDF, 3M Unitek, Monrovia, CA, USA). The initial oxidation treatment followed the instructions of the alloy manufacturer, and the subsequent firing cycles followed the recommendations for IPS Classic porcelain (Ivoclar Vivadent). All specimens for fatigue testing received the full heat-treatment regimen for porcelain application.

Table 2 Mechanical properties reported by manufacturer (simulated heat treatment for porcelain application)[a]

Alloy	0.2% Yield strength (MPa)	Vickers hardness	Elongation (%)
IS 64	560	230	31.0
d.SIGN 59	490	230	14.0

[a] Ivoclar Vivadent, Amherst, NY, USA

Table 1 Nominal compositions of alloys provided by manufacturer[a]

Alloy	Pd	Ag	Sn	Zn	In	Au	Pt	Cu	Ga	Ru	Ir	Re	Other
IS 64	59.9	26.0	7.0	–	1.5	2.8	1.0	–	1.8	<1.0	–	<1.0	–
d.SIGN 59	59.2	27.9	8.2	1.3	2.7	–	<1.0	–	–	<1.0	–	<1.0	Li < 1.0

[a] Ivoclar Vivadent, Amherst, NY, USA

Fatigue tests were performed in air at room temperature, using uniaxial sinusoidal tension–compression loading with a servohydraulic mechanical testing machine (Model 1322, Instron Corp., Canton, MA, USA). The ratio (R) between tensile and compressive stress amplitudes was −1, and the frequency was 10 Hz. Starting stress amplitudes were based on previous experience with high-Pd [23] and Pd–Ag [24] alloys, which resulted in the need for considerably fewer specimens than with conventional staircase methods [27, 28]. Two replicate specimens were tested at each stress amplitude, and the highest stress at which fracture did not occur after a clinically relevant number [29] of 2×10^6 cycles was designated as the fatigue limit. Fracture surfaces of fatigued specimens were examined with a scanning electron microscope (SEM) (JSM-820, JEOL Ltd, Tokyo, Japan) over a range of magnifications. Before SEM examination, these specimens were ultrasonically cleaned in ethanol.

Microstructural observations were carried out with the same SEM on the coping specimens in both the as-cast and heat-treated conditions, and on specimens from the fractured fatigue test bars (axial and longitudinal). Both types of metallographic specimens were first obtained by sectioning with the use of a slow-speed water-cooled diamond saw. Specimens were mounted in transparent epoxy resin (Leco, St. Joseph, MI, USA). After grinding with 320, 400, and 600 grit silicon carbide papers, and polishing with a series of gamma-alumina slurries ending with 0.05 μm particles, specimens were etched in aqua regia solutions, using appropriate times to obtain optimum microstructures. Porosity evaluation was conducted on fatigue fracture surfaces and on samples sectioned both axially (about 3 mm from fracture surface) and longitudinally from fatigue test specimens, using the SEM and an optical microscope (Nikon Epiphot, Nippon Kogaku K.K., Japan). The preparation method for the samples was the same as that of specimens for microstructural observation, except that these samples were not etched. Image analysis was completed using special software (ImageJ 1.34, National Institutes of Health, Bethesda, MD, USA). An equivalent pore diameter D_e [30, 31] was used to describe the size of near-spherical or irregular shape pores, which is defined here as $D_e = 2[A_p/\pi]^{1/2}$ with A_p the pore area measured directly from metallographic samples or fatigue fracture surfaces.

Vickers hardness (M-400, Leco Corp, St. Joseph, MI, USA) was measured on etched specimens, using a 1 kg load and dwell time of 30 s. Mean hardness values were obtained from 5 indentations. Analysis of variance (ANOVA) at the $\alpha = 0.05$ level was used to determine if significant differences in hardness existed between (a) as-cast and heat-treated specimens of the same alloy, (b) the two alloys in the as-cast or heat-treated condition, and (c) coping specimens and fatigue test specimens of the same alloy in the heat-treated condition.

3 Results

3.1 Microstructures

Microstructures of as-cast and heat-treated coping specimens are respectively shown in Fig. 1a and b for IS 64, and in Fig. 1c and d for d.SIGN 59. The as-cast microstructures of both alloys were inhomogeneous. After simulated porcelain firing heat treatment, the microstructures of the coping specimens were homogenized and contained numerous precipitates, along with the palladium solid solution matrix. Microstructures of heat-treated fatigue test specimens are shown in Fig. 2a and b. Compared to the heat-treated coping specimens for IS 64 and d.SIGN 59, the much larger heat-treated fatigue test specimens still had incompletely homogenized microstructures. Compositions of the palladium solid solution and the Pd–Ag–Sn–In precipitates in another Pd–Ag alloy have been obtained by x-ray energy-dispersive spectroscopy (EDS) with the transmission electron microscope [32]. The matrix and precipitates in IS 64 and d.SIGN 59 are expected to have similar compositions.

3.2 Vickers hardness

Table 3 summarizes the Vickers hardness measurements for the as-cast and heat-treated coping specimens and the heat-treated fatigue test specimens for the IS 64 and d.SIGN 59 alloys. The results of statistical comparisons using ANOVA are presented in Tables 4 and 5. There was no significant difference in Vickers hardness of the coping specimens for the two alloys in either the as-cast condition or the simulated porcelain-firing heat-treated condition. However, after heat treatment, the Vickers hardness of the coping specimens fabricated from each alloy decreased significantly, compared to the as-cast condition. The Vickers hardness of the heat-treated fatigue test specimens was significantly higher than that of the heat-treated coping specimens which had much smaller dimensions. The Vickers hardness for the heat-treated fatigue test specimens fabricated from both alloys were quite close to the value (230) provided by the manufacturer for the porcelain-fired heat-treated condition (Table 2).

3.3 Fatigue limits

Table 6 lists the number of cycles to failure at different stress amplitudes for IS 64 and d.SIGN 59. Because the fatigue limit of cast Pd-based dental alloys is sharply

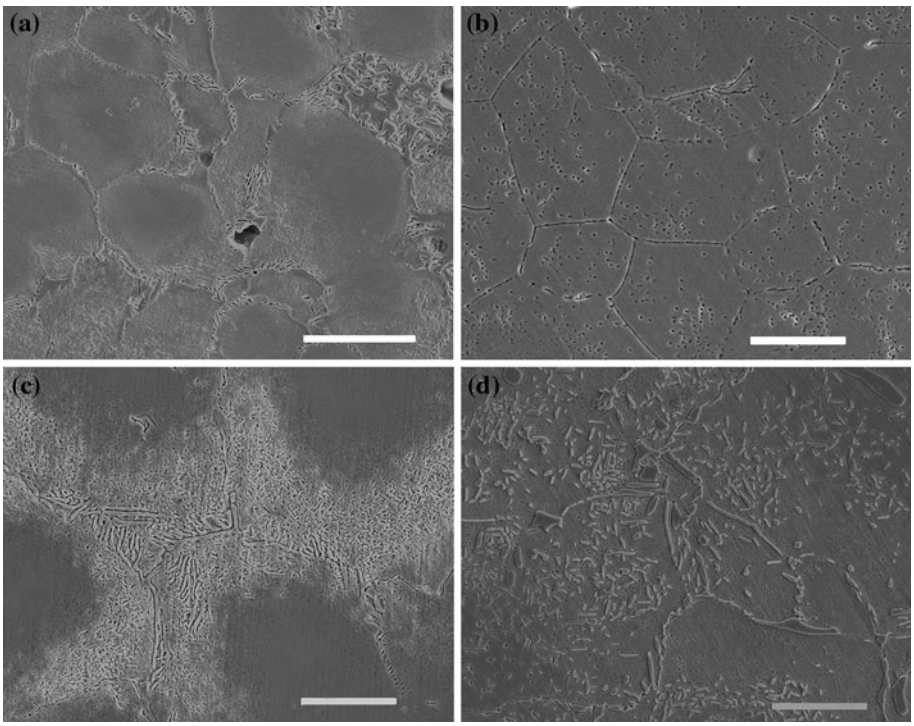

Fig. 1 SEM images showing the microstructures of (**a**) as-cast and (**b**) heat-treated IS 64 coping specimens, and (**c**) as-cast and (**d**) heat-treated d.SIGN 59 coping specimens. Length of scale bar = 15 μm for (**a**), and 10 μm for (**b**–**d**)

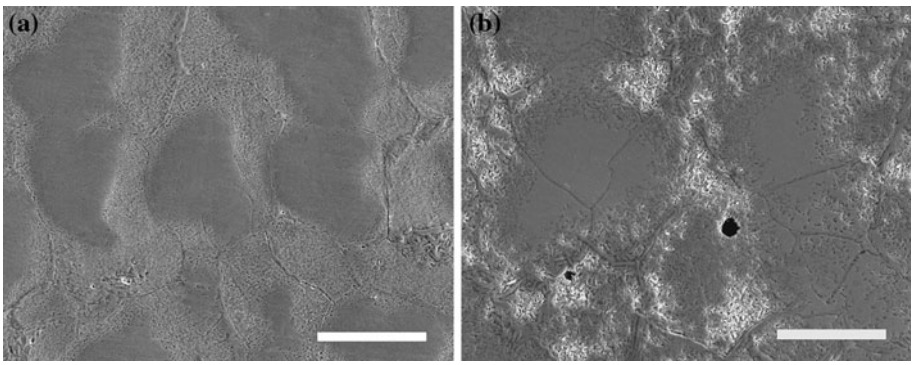

Fig. 2 SEM images showing the incompletely homogenized microstructures in fatigue test specimens after simulated porcelain-firing heat treatment for (**a**) IS 64 and (**b**) d.SIGN 59. Length of scale bar = 30 μm for (**a**) and 20 μm for (**b**)

Table 3 Vickers hardness (VHN) for copings and fatigue test specimens

Alloy	As-cast copings	Heat-treated copings	Fatigue test specimens (Heat-treated)
IS 64	237 (8.8)	201 (7.3)	224 (10.3)
d.SIGN 59	244 (7.3)	206 (9.9)	229 (3.6)

Data are mean values (standard deviations). Heat treatment simulated application of dental porcelain

Table 4 Statistical comparisons of Vickers hardness between as-cast and heat treated coping specimens, using two-way ANOVA

Source	Degrees of freedom	Sum of squares	Mean square	*F*-value	*P*-value
Alloy	1	409.657	409.657	43.730	0.096
Condition	1	13752.528	13752.528	1468.065	0.017
Alloy × condition	1	9.368	9.368	0.132	0.718
Error	36	2546.482	70.736		

dependent upon stress amplitude [23, 24], the fatigue limit of IS 64 is close to 0.20 of its 0.2% yield strength, while the fatigue limit of d.SIGN 59 is close to 0.25 of its 0.2% yield strength. The representative fracture surface of an IS 64 fatigue specimen in Fig. 3 shows the substantial casting porosity that was observed on the fracture surfaces of all fatigue specimens.

Table 5 Statistical comparisons of Vickers hardness between heat-treated coping specimens and fatigue test specimens, using two-way ANOVA

Source	Degrees of freedom	Sum of squares	Mean square	*F*-value	*P*-value
Alloy	1	266.779	372.798	2.798	0.033
Specimen type	1	5307.695	7417.015	7417.015	0.007
Alloy × specimen type	1	0.716	0.716	0.011	0.919
Error	36	2439.738	67.770		

Table 6 Number of cycles to failure for IS 64 and d.SIGN 59 specimens tested at different stress amplitudes

Specimen no.	Alloy	Stress amplitude	Cycles to failure
1	IS 64	0.15 $\sigma_{0.2}$ (84 MPa)	>2,000,000
2		0.15 $\sigma_{0.2}$ (84 MPa)	–[a]
3		0.20 $\sigma_{0.2}$ (112 MPa)	1,350,751
4		0.20 $\sigma_{0.2}$ (112 MPa)	1,651,575
5	d.SIGN 59	0.20 $\sigma_{0.2}$ (98 MPa)	>2,000,000
6		0.20 $\sigma_{0.2}$ (98 MPa)	>2,000,000
7		0.25 $\sigma_{0.2}$ (123 MPa)	>2,000,000
8		0.25 $\sigma_{0.2}$ (123 MPa)	405,874[b]

[a] Specimen 2 was inadvertently damaged during the initial set-up before the cyclic fatigue testing began

[b] The anomalously low number of cycles to failure for Specimen 8, compared to Specimen 7, was attributed to excessive surface porosity

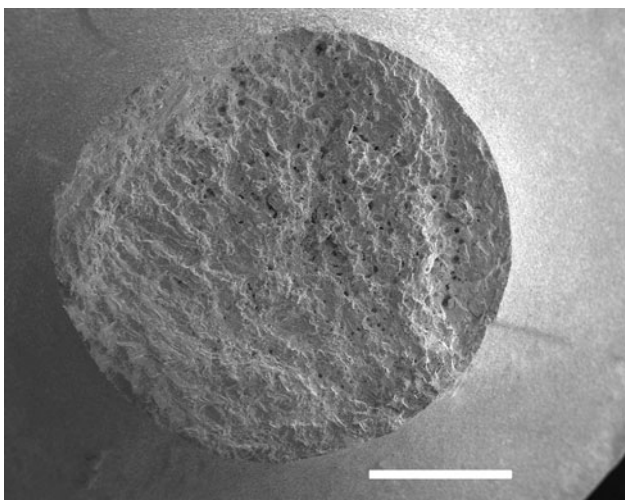

Fig. 3 SEM image showing fracture surface with unevenly distributed casting porosity in IS 64 specimen that failed at 1,651,575 cycles. Length of scale bar = 1 mm

3.4 Casting porosity and fracture characteristics

Numerous unevenly distributed casting pores were observed in all fatigue test specimens, with a tendency to segregate along the fracture surface and cross-section of the specimens, as shown in the series of optical microscope photographs from a sectioned d.SIGN 59 fatigue test specimen in Fig. 4. IS 64 specimens exhibited less porosity than d.SIGN 59 specimens. The porosity in one d.SIGN 59 fatigue test specimen (Specimen 8 in Table 6) was particularly substantial with an overall pore area percentage of 12% and maximum equivalent pore diameter of 280 μm. In this specimen, near-surface porosity was considered to be the cause of fracture at a low number of 405,874 cycles with 0.25 $\sigma_{0.2}$. Among all other specimens, the overall pore area percentage was not more than 5% in IS 64 and 10% in d.SIGN 59. The maximum equivalent pore diameter in IS 64 and d.SIGN 59 specimens was observed to be 85 μm (Specimen 4 in Table 6, fractured at 1,651,575 cycles) and 150 μm (Specimen 7 in Table 6, survived 2 million cycles), respectively. Figure 4 shows the casting pore distribution on the cross-sectioned and polished surface of this latter d.SIGN 59 fatigue specimen. It is noteworthy that such relatively large and widely separated casting pores could be tolerated in the bulk regions of these relatively large test specimens without serious degradation of the fatigue properties.

On the complex fatigue fracture surfaces, fatigue crack initiation sites were not uniformly determined, being located either near the specimen surface or inside the specimen, or with multiple locations. Fatigue striations [23, 24] were observed on the fracture surfaces of IS 64 and d.SIGN 59. The local orientation of the striations changed in IS 64, as shown in Fig. 5a, but this change was not observed in the fracture surface of d.SIGN 59, as shown in Fig. 5b.

4 Discussion

4.1 Specimen size and microstructures

The speed of liquid metal solidification is very high during conventional dental casting, and the microstructures of as-cast high-Pd alloys can deviate substantially from their equilibrium microstructures [33]. During the porcelain firing process, the as-cast microstructures of the Pd–Ag alloy generally become homogenized, as shown in Fig. 1. For the relatively large tensile test specimens (identical to those used in the fatigue tests) of one high-Pd alloy, Spartan Plus (Ivoclar Vivadent, Amherst, NY, USA), the as-cast dendritic microstructure was not completely eliminated by porcelain-firing heat treatment [25]. Moreover, the near-surface eutectic constituent [33] in as-cast coping specimens of the high-Pd alloy Liberty (Heraeus Kulzer, Armonk, NY, USA) was not observed in the much larger as-cast tensile test specimens [25]. These examples

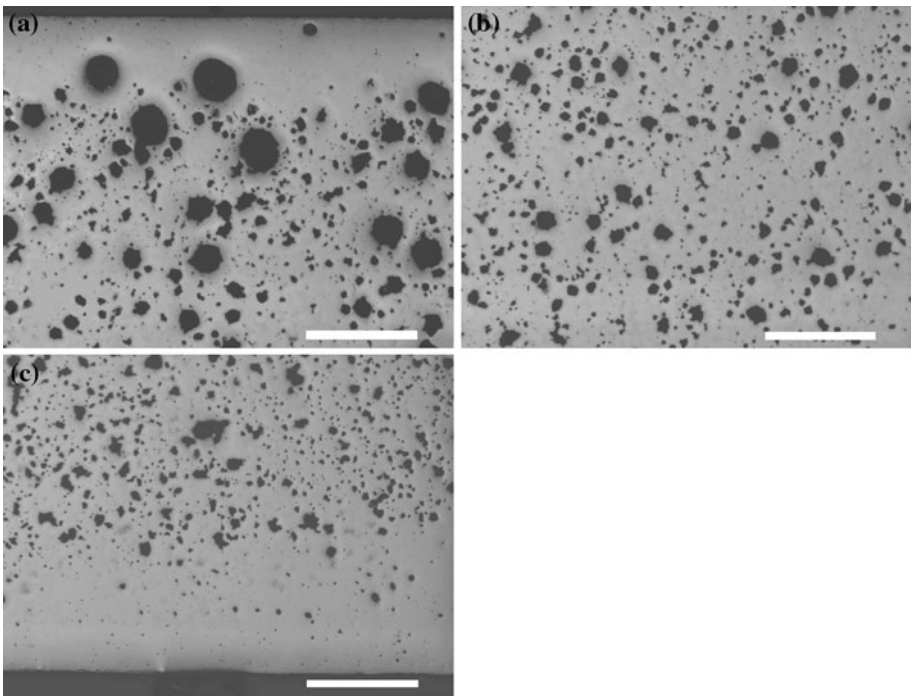

Fig. 4 Optical micrographs showing casting porosity in longitudinally cross-sectioned d.SIGN 59 specimen that survived 2 million cycles: (**a**) and (**c**) are from regions near two opposite surfaces; (**b**) is from central region. Length of scale bar = 400 μm

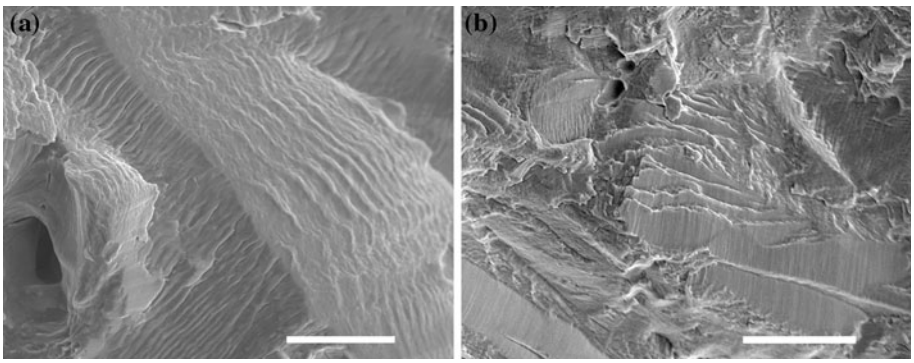

Fig. 5 SEM images showing fatigue striations on the fracture surfaces of (**a**) IS 64 specimen that failed at 1,651,575 cycles and (**b**) d.SIGN 59 specimen that failed at 405,874 cycles. Length of scale bar = 10 μm for (**a**) and 15 μm for (**b**)

illustrate the great importance of casting thickness, which controls the rate of heat flow from the solidifying alloy, on as-cast microstructure of the high-Pd alloys.

Similar observations were made for the Pd–Ag alloys in this study, in which the microstructures of the relatively large fatigue test specimens for both alloys were not homogenized after the porcelain firing heat treatment, as shown in Fig. 2. Therefore, the effect of the test specimen dimensions for the Pd–Ag alloy on the resulting as-cast and heat-treated microstructures cannot be ignored. The incomplete homogenization of the heat-treated fatigue specimens is considered to account for their higher Vickers hardness (Table 3) compared to the heat-treated coping specimens where the microstructures were homogenized. Consequently, the data for mechanical properties obtained with relatively large test specimens with dimensions meeting ADA specification requirements [21, 22] may not accurately reflect the mechanical properties of clinical restorations.

4.2 Comparison of fatigue properties for IS 64 and d.SIGN 59

The compositions of IS 64 and d.SIGN 59 are very similar, with only small differences in the percentages of component elements (Table 1). However, the microstructures of the two alloys are quite different (Figs. 1 and 2). Moreover, the 0.2% yield strength of IS 64 is over 10% higher than that of d.SIGN 59, while the ductility (percentage elongation) of IS 64 is twice that of d.SIGN 59 (Table 2). These general results are typical for the Pd–Ag dental alloys, where compositions differing by only small percentages for the component elements can have substantially different mechanical properties [15].

In the present study the fatigue limit of d.SIGN 59 appears to be 10% greater than that of IS 64 (Table 6), which is inconsistent with previous observations that the high-Pd or Pd–Ag alloy with higher yield strength exhibits

higher fatigue limit [23, 24]. The difference in fatigue performance for IS 64 and d.SIGN 59 can be attributed to microstructural differences and the mechanisms for fatigue fracture. For example, the variation of fatigue striation orientation in IS 64, shown in Fig. 5a, suggests relative ease of fatigue crack initiation at multiple sites and/or relative ease of fatigue crack propagation in this alloy. Determination of the detailed mechanisms for fatigue crack initiation and propagation in these Pd–Ag alloys requires further study.

4.3 Effects of specimen size and casting porosity on fatigue performance

Experience in engineering has shown that in most cases a specimen size effect on fatigue performance exists, and two factors can result from change in fatigue specimen size: (a) the change in surface area and (b) the variation of stress gradient across the specimen diameter and the volume of material that is highly stressed [34]. Since specimen size effects on microstructures can occur for Pd-based dental alloy castings, it is important to have a standardized protocol for fatigue testing that provides performance information relevant to fatigue conditions for clinical restorations. Such a standardized tensile test or fatigue test for specimens having the dimensions of typical metal-ceramic restorations remains to be developed.

During practical dental casting processes, casting defects such as pores and microshrinkage, cannot be completely eliminated [35, 36]. Casting porosity in steels, engineering aluminum and magnesium alloys has been reported to be preferential fatigue crack initiation sites and constitute the main influence on fatigue properties [30, 31, 37–44]. A cast Ag–Pd–Cu–Au–Zn alloy for dental applications has been found to have considerably smaller fatigue strength than the drawn Ag–Pd–Cu–Au–Zn alloy [36, 45]. Although quantitative approaches [30, 31, 36–40, 45] have been made to predict the relation between fatigue life and casting porosity, there is no well accepted method to predict the effects of porosity on fatigue life.

Important measures of casting porosity include morphology, size, density and fraction of pores. Under cyclic stresses, high stress concentration around sharp porosity can be released by localized plastic deformation and thus the shape effect of pores on fatigue performance can be negligible [31]. The present results indicate that specimens with many pores in both IS 64 and d.SIGN 59 survived 2 millions cycles, while only one d.SIGN 59 specimen with severe casting porosity fractured after an expectedly low number of cycles (specimen 8 in Table 6, with total pore area percentage of 12% and a maximum equivalent pore diameter of 280 μm). This suggests that in the present Pd–Ag alloys there exists a critical pore size, below which the alloys exhibit fatigue tolerance to the pores. Similar pore size affects on fatigue have been reported in cast aluminum and magnesium alloys [31, 38–41, 43, 44] and in Ag-Pd alloys [36, 45]. The present microstructural analysis shows that the critical pore size is approximately on the order of 150 μm for d.SIGN 59 and 85 μm for IS 64. The corresponding critical stress intensity amplitude K_{cr} can be roughly calculated using the following equation [39]:

$$K_{cr} = \sigma_{cr}\alpha[\pi A_p^{1/2}]^{1/2} \quad (1)$$

where σ_{cr} is the critical stress amplitude and here can be correlated to fatigue limit [38]; A_p is the area of the pore with maximum equivalent pore diameter, which was measured on the metallographic or fatigue fracture surface; $\alpha = 0.65$ for surface cracks and $\alpha = 0.50$ if the cracks originate from internal porosity. As both experimental observation and finite element analysis indicated that large pores close to or at the specimen surface induce higher stress/strain concentration than other pores [30, 31], pores at or near the surface were considered to simplify calculation. The critical stress intensity amplitude was calculated to be approximately 1.12 and 1.63 MPa $m^{1/2}$ for IS 64 and d.SIGN 59, respectively, which are quite close to the critical stress intensity amplitude values [39] in casting magnesium alloys. When the size of casting pores is less than the critical pore size, the critical stress intensity amplitude is below long crack threshold stress intensity. In such case, even though fatigue cracks may initiate at porosity, they will not propagate to cause fatigue failure. Therefore, these pores are in non-propagating conditions [38] and thus tolerable for fatigue performance. It should be noted that the effective cross-section reduction due to the existence of one pore with critical pore size and the resulting rise in overall mean stress inside the specimen is considerably small. However, if many pores with comparable size aggregate in the same cross-section, the rise in overall mean stress in the specimen will be significant. Characterization of the locations and distribution of casting pores and an investigation of the effects of casting porosity on fatigue properties of Pd–Ag alloys are strongly recommended for future research. The casting porosity in these alloys, along with their complex microstructures, should be directly related to their relatively low ratios of fatigue limit to yield strength.

5 Conclusions

This was the first investigation to consider in detail the effect of casting porosity on fatigue behavior of dental alloys. Two Pd–Ag alloys (IS 64 and d.SIGN 59) of similar compositions, but differing microstructures and mechanical properties, were selected for study. The Pd–Ag alloys are

particularly susceptible to the development of casting porosity. Under the conditions of the present study, the following conclusions can be drawn:

1. While the microstructures of as-cast IS 64 and d.SIGN 59 coping specimens representative of dental restorations were inhomogeneous, after simulated porcelain-firing heat treatment these microstructures were substantially homogenized with the formation of numerous precipitates.
2. In comparison with the heat-treated coping specimens, the much larger heat-treated fatigue test specimens of the two alloys had incompletely homogenized microstructures.
3. There was no significant difference in Vickers hardness between the IS 64 and d.SIGN 59 coping specimens for the as-cast condition and for the heat-treated condition. After the simulated porcelain-firing heat treatment, significant decreases occurred in the Vickers hardness of the coping specimens prepared from the two alloys. The Vickers hardness of the heat-treated fatigue test specimens was significantly higher than that of the heat-treated coping specimens.
4. The fatigue limit of IS 64 is close to 0.20 of its 0.2% yield strength, while the fatigue limit of d.SIGN 59 is close to 0.25 of its 0.2% yield strength. The relative values of fatigue limit for these two alloys are reversed from the relative values of yield strength, suggesting differences in fatigue crack initiation and propagation at the microstructural level. The relatively low ratio of fatigue limit and yield strength for the Pd–Ag alloys is attributed to their complex microstructures as well as to casting porosity.
5. While casting porosity was observed in all fatigue test specimens, the fatigue limit was not further reduced from the range of 0.20–0.25 of the 0.2% yield strength until a critical pore size was reached in the alloys, approximately 85 μm for IS 64 and 150 μm for d.SIGN 59.
6. Further extensive study of the fine-scale microstructures and precipitate compositions in the coping and fatigue test specimens with the transmission electron microscope is recommended to complement the present SEM observations.

Acknowledgments This study was supported by Grant DE 10147 from the National Institutes of Dental and Craniofacial Research of the National Institute of Health, Bethesda, MD, USA. We would like to thank Lloyd Barnhart in the Department of Materials Science and Engineering for his expert technical assistance in the fatigue testing and Tridib Dasgupta, Director of Materials Research and Development, Ivoclar Vivadent, for his research support and constructive comments.

References

1. Goodacre CJ. Palladium–silver alloys: a review of the literature. J Prosthet Dent. 1989;62:34–7.
2. Huget EF, Civjan S. Status report on palladium–silver-based crown and bridge alloys. J Am Dent Assoc. 1974;89:383–5.
3. Bertolotti RL. Selection of alloys for today's crown and fixed partial denture restorations. J Am Dent Assoc. 1984;108:959–66.
4. Huget EF, Dvivedi N, Cosner HE. Characterization of gold–palladium–silver and palladium–silver for ceramic–metal restorations. J Prosthet Dent. 1976;36:58–65.
5. Limkool P, Sumii T. Study of a Pd–Ag–Sb system alloy for metal-ceramics. Bull Tokyo Dental Coll. 1995;36:103–14.
6. Bertolotti RL. Alternative casting alloys for today's crown and bridge restorations. Part II: metal-ceramic restorations. J Calif Dent Assoc. 1983;11:63–9.
7. Compton HK, Lacefield WR, O'Neal SJ. Marginal fit evaluation of palladium alloys vs a gold alloy. J Dent Res. 1985;64:317. [Abstract].
8. Papazoglou E, Brantley WA, Johnston WM. Evaluation of high-temperature distortion of high-palladium metal-ceramic crowns. J Prosthetic Dent. 2001;85:133–40.
9. Reel DC, Kemper JT, Jones WB, Mitchell RJ. A clinical comparison of Au–Pd and Pd–Ag PFM alloys. J Dent Res. 1986;65:237. [Abstract].
10. Mezger PR, Stols AL, Vrijhoef MM, Greener EH. Metallurgical aspects of palladium–silver porcelain–bonding alloys. J Dent. 1989;17:90–3.
11. Papazoglou E, Brantley WA. Porcelain adherence vs force to failure for palladium–gallium alloys: a critique of metal–ceramic bond testing. Dent Mater. 1998;14:112–9.
12. Canay S, Oktemer M. In vitro corrosion behavior of 13 prosthodontic alloys. Quintessence Int. 1992;23:279–87.
13. Mezger PR, Vrijhoef MMA, Greener EH. The corrosion behavior of palladium–silver–ceramic alloys. Dent Mater. 1989;5:97–100.
14. Sun D. Ph.D. Dissertation. Columbus: The Ohio State University; 2004.
15. Brantley WA, Laub LW. Metal selection. In: Rosenstiel SF, Land MF, Fujimoto J, editors. Contemporary fixed prosthodontics. 4th ed. St. Louis: Mosby/Elsevier; 2006. p. 598–609.
16. Bertolotti RL. Rational selection of casting alloys. In: Preston JD, editor. Perspectives in dental ceramics. Proceedings of the Fourth International Symposium on Ceramics. Chicago: Quintessence; 1988. p. 75–84.
17. Lacy AM, Hirose R, Jendresen MD. Observation on the discoloration of low-fusing porcelain. J Calif Dent Assoc. 1977;5:44–9.
18. Stavridakis MM, Papazoglou E, Seghi RR, Johnston WM, Brantley WA. Effect of different high-palladium metal-ceramic alloys on the color of opaque and dentin porcelain. J Prosthetic Dent. 2004;92:170–8.
19. O'Brien WJ, Boenke KM, Linger JB, Groh CL. Cerium oxide as a silver decolorizer in dental porcelains. Dent Mater. 1998;14:365–9.
20. Ringle RD, Mackert JR, Fairhurst CW. Prevention of porcelain "greening" by external oxidation in a Pd–Ag–Mn–Al dental alloy system. J Dent Res. 1986;65:218. [Abstract].
21. American National Standard/American Dental Association Specification No. 5 for dental casting alloys. Chicago: American Dental Association; 1997.
22. American National Standard/American Dental Association Specification No. 38 for metal-ceramic dental restorative systems. Chicago: American Dental Association; 2000.
23. Li D, Brantley WA, Mitchell JC, Daehn GS, Monaghan P, Papazoglou E. Fatigue studies of high-palladium dental casting

alloys: Part I. Fatigue limits and fracture characteristics. J Mater Sci Mater Med. 2002;13:361–7.
24. Li D, Brantley WA, Guo W, Clark WAT, Alapati SB, Heshmati RH, Daehn GS. Fatigue limits and SEM/TEM observations of fracture characteristics for three Pd–Ag dental casting alloys. J Mater Sci Mater Med. 2007;18:119–25.
25. Papazoglou E, Wu Q, Brantley WA, Mitchell JC, Meyrick G. Comparison of mechanical properties for equiaxed fine-grained and dendritic high-palladium alloys. J Mater Sci Mater Med. 2000;11:601–8.
26. Vermilyea SG, Cai Z, Brantley WA, Mitchell JC. Metallurgical structure and microhardness of four new palladium-based alloys. J Prosthodont. 1996;5:288–94.
27. ASTM Committee E-9. A guide for fatigue testing and the statistical analysis of fatigue data. ASTM Special Technical Publication No. 91-A. 2nd ed. Philadelphia: American Society for Testing and Materials; 1963.
28. Collins JA. Fatigue of materials in mechanical design: analysis, prediction, and prevention. 2nd ed. New York: Wiley; 1993. p. 383–92.
29. Anselm Wiskott HW, Nicholls JI, Belser UC. Stress fatigue: basic principles and prosthodontic implications. Int J Prosthodont. 1995;8:105–16.
30. Yi JZ, Gao YX, Lee PD, Flower HM, Lindley TC. Scatter in fatigue life due to effects of porosity in cast A356-T6 aluminum–silicon alloys. Metall Mater Trans. 2003;34A:1879–90.
31. Gao YX, Yi JZ, Lee PD, Lindley TC. The effect of porosity on the fatigue life of cast aluminum–silicon alloys. Fatigue Fract Eng Mater Struct. 2004;27:559–70.
32. Guo WH, Brantley WA, Clark WA, Monaghan P, Mills MJ. Transmission electron microscopic investigation of a Pd–Ag–In–Sn dental alloy. Biomaterials. 2003;24:1705–12.
33. Brantley WA, Cai Z, Carr AB, Mitchell JC. Metallurgical structures of as-cast and heat-treated high-palladium dental alloys. Cells Mater. 1993;3:103–14.
34. Dieter GE. Mechanical metallurgy. 3rd ed. New York: McGraw-Hill; 1986. p. 406–7.
35. Anusavice KJ. Phillips' science of dental materials. 11th ed. St. Louis: Saunders/Elsevier; 2003. p. 342–7.
36. Mizumoto T, Niinomi M, Akahori T, Fuhui H. Effects of casting defects and microstructure on fatigue properties of cast Ag–Pd–Cu–Au–Zn alloys for dental applications. Mater Sci Forum. 2003 [Part 4, THERMEC] 426–32:3207–12.
37. Sigl KM, Hardin RA, Stephens RI, Beckermann C. Fatigue of 8630 cast steel in the presence of porosity. Int J Cast Metals Res. 2004;17:130–46.
38. Mayer H, Papakyriacou M, Zettl B, Vacic S. Endurance limit and threshold stress intensity of die cast magnesium and aluminum alloys at elevated temperatures. Int J Fatigue. 2005;27:1076–88.
39. Mayer H, Papakyriacou M, Zettl B, Stanzl-Tschegg SE. Influence of porosity on the fatigue limit of die cast magnesium and aluminium alloys. Int J Fatigue. 2003;25:245–56.
40. Wang QG, Apelian D, Lados DA. Fatigue behavior of A356-T6 aluminum cast alloys. Part I. Effect of casting defects. J Light Metals. 2001;1:73–84.
41. Mayer HR, Lipowsky H, Papakyriacou M, Rosch R, Stich A, Stanzl-Tschegg S. Application of ultrasound for fatigue testing of lightweight alloys. Fatigue Fract Eng Mater Struct. 1999;22:591–9.
42. Stanzl-Tschegg SE, Mayer HR, Beste A, Kroll S. Fatigue and fatigue crack propagation in AlSi7Mg cast alloys under in-service loading conditions. Int J Fatigue. 1995;17:149–55.
43. Horstemeyer MF, Yang N, Gall K, McDowell D, Fan J, Gullett P. High cycle fatigue mechanisms in a cast AM60B magnesium alloy. Fatigue Fract Eng Mater Struct. 2002;25:1045–56.
44. Buffiere JY, Savelli S, Jouneau PH, Maire E, Fougeres R. Experimental study of porosity and its relation to fatigue mechanisms of model Al–Si7–Mg0.3 cast Al alloys. Mater Sci Eng. 2001;A316:115–26.
45. Mizumoto T, Niinomi M, Nakano Y, Akahori T, Fukui H. Fatigue properties of cast Ag–Pd–Cu–Au–Zn alloy for dental applications in the relation with casting defects. Mater Trans. 2002; 43:3160–6.